

Simple 2-D Direction-of-Arrival Estimation Using an ESPAR Antenna

Lukasz Kulas, *Senior Member, IEEE*

Abstract—In this letter, it has been shown how an electronically steerable parasitic array radiator (ESPAR) antenna can be used for 2-D direction-of-arrival (DoA) estimation employing received signal strength (RSS) values only. The proposed approach relies on changes in RSS values recorded at the antenna output port observed for different vertical and horizontal directions, while antenna's main beam sweeps 360° area around the ESPAR antenna. Based on the observed diversity in RSS values, obtained for different ESPAR antenna radiation patterns and different directions of a signal impinging the antenna, a simple 2-D DoA estimator has been proposed. Measurements using the fabricated ESPAR antenna indicate that, by relying solely on RSS values and the proposed algorithm, it is possible to perform 2-D DoA estimation with the acceptable accuracy in realistic and inexpensive systems, where the phase of impinging signals cannot easily be measured.

Index Terms—Direction of arrival (DoA), electronically steerable parasitic array radiator (ESPAR) antenna, received signal strength (RSS), switched-beam antenna, 2-D DoA estimation.

I. INTRODUCTION

DIRECTION-OF-ARRIVAL (DoA) estimation is an important technique used to determine the direction of a radio frequency (RF) signals impinging an antenna array. Algorithms for DoA estimation are used commonly in a number of wireless systems applications, e.g., to localize objects or to improve the performance of wireless networks that may be influenced by other RF sources [1], [2]. The most common approach for 2-D DoA estimation, which includes simultaneous determination of both horizontal and elevation angles, involves adaptive antenna arrays together with dedicated algorithms for processing signals received by all antenna elements [1]. However, involvement of multiple receivers in a single DoA system results in high overall costs, which limits possible applications of such systems.

Electronically steerable parasitic array radiator (ESPAR) antennas are single-port output structures, where a single radiating element is surrounded by a number of parasitic elements ended

Manuscript received June 21, 2017; accepted July 14, 2017. Date of publication July 31, 2017; date of current version August 28, 2017. This work was conducted within the ENABLE-S3 project that received funding from the ECSEL Joint Undertaking under Grant 692455. This Joint Undertaking received support from the European Union's HORIZON 2020 research and innovation program and Austria, Denmark, Germany, Finland, Czech Republic, Italy, Spain, Portugal, Poland, Ireland, Belgium, France, The Netherlands, The U.K., Slovakia, and Norway. (Corresponding author: Lukasz Kulas.)

The author is with the Department of Microwave and Antenna Engineering, Faculty of Electronics, Telecommunications and Informatics, Gdansk University of Technology, 80-233 Gdańsk, Poland (e-mail: lukasz.kulas@eti.pg.gda.pl).

Color versions of one or more of the figures in this letter are available online at <http://ieeexplore.ieee.org>.

Digital Object Identifier 10.1109/LAWP.2017.2728322

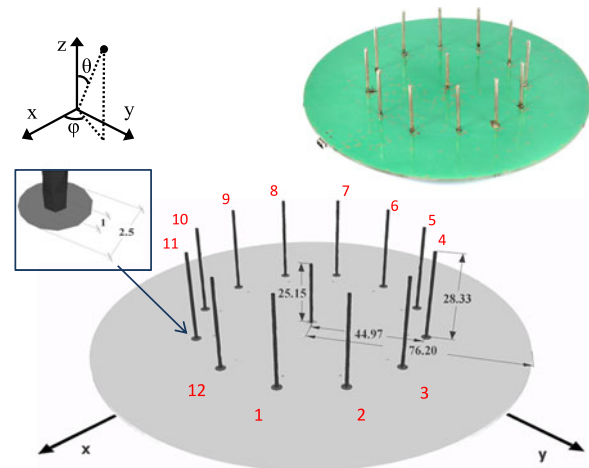


Fig. 1. Fabricated ESPAR antenna with its dimensions (in mm) and numbering of the parasitic elements. Horizontal angles corresponding to the elements' positions are equal to $\varphi = n \cdot 30^\circ$, where n is the element's number.

up with reactances that can be controlled electronically [3]–[5]. For different values of the reactances connected to the parasitic elements, one can obtain different radiation patterns that consequently may also be changed electronically.

The ability to generate different radiation patterns by an ESPAR antenna electronically has been used by many authors to estimate DoA of an impinging signal [1], [5]–[8]. Although high-accuracy algorithms for ESPAR antenna-based systems have been introduced already [5], [6], the research, which has been conducted by over a decade, has focused almost entirely on 1-D (horizontal plane) DoA estimation. This focus is understandable as it is well aligned with the natural behavior of ESPAR antennas—the highest diversity in electronically changed radiation patterns is available in the horizontal plane, i.e., $\theta = 90^\circ$ plane in Fig. 1 [5], [6].

Thus far, only one attempt has been made in order to provide a full 2-D DoA estimation using an ESPAR antenna [7]. The authors have proposed a simple projection of the 2-D DoA problem onto the horizontal plane assuming simplified ESPAR antenna radiation patterns and not involving any electromagnetic relations between the antenna elements. In consequence, although the authors have performed simulations of 2-D DoA estimation, where both horizontal and elevation angles were determined simultaneously, the calculation of vertical angles has been possible only due to simplification they have used. Hence, no evidence exists that the method proposed in [7] is

applicable to realistic ESPAR antenna designs. Moreover, no received signal strength (RSS)-based 2-D DoA estimators have been proposed thus far.

In this letter, a new algorithm for 2-D DoA estimation for ESPAR antennas is introduced and verified in measurements. The proposed method relies on observations of how 3-D ESPAR antenna radiation patterns change in both vertical and horizontal directions. The algorithm relies on RSS values only; therefore, it can easily be applied in simple and inexpensive devices for 2-D DoA estimation, where the phase of impinging signals cannot easily be measured.

II. ANALYSIS OF ESPAR ANTENNA RADIATION PATTERNS FOR A SIMPLE RSS-BASED 2-D DOA ESTIMATION

A. ESPAR Antenna

To observe the changes in radiation patterns of an ESPAR antenna across horizontal and elevation planes, a fabricated prototype of the design proposed in [8] with 12 parasitic elements has been used. The antenna, presented in Fig. 1, uses 1.7-mm-high FR4 laminate with a top-layer metallization being its ground plane and has a center active monopole fed by an SMA connector. The parasitic elements are ended by NJG1681MD7 SPDT (single-pole, double-throw) switches. Hence, every element can be connected to the ground or opened electronically, making all parasitic elements, which have been connected to the ground, reflectors, while those opened become directors. In consequence, the associated antenna configuration can be denoted by the steering vector $V = [v_1, v_2, \dots, v_{12}]$, where v_n can take values 0 or 1 when the n th element is, respectively, connected to the ground or opened.

The antenna's input reflection coefficient, better than -14 dB, has been measured at the frequency 2.484 GHz for every configuration having the narrowest directional main beam in the horizontal direction, which, as in the design in [8], has been obtained for seven consecutive parasitic elements shortened to the ground.

B. Analysis of the ESPAR Antenna Radiation Patterns in Horizontal and Vertical Planes

The key factor enabling accurate 1-D DoA horizontal angle estimation is high diversity in radiation patterns of an ESPAR antenna in the horizontal plane for different main beam directions. To analyze this effect, let us consider a 3-D radiation pattern shown in Fig. 2, which has been obtained from FEKO electromagnetic simulation for the designed antenna (see Fig. 1). In the radiation pattern presented in Fig. 2, which corresponds to the configuration defined by the steering vector $V_{\max}^1 = [1, 1, 1, 1, 1, 0, 0, 0, 0, 0, 0, 0]$, the directional main beam has 3-dB beamwidth that equals 73.2° and 61.8° in, respectively, horizontal and vertical directions with the maximum for $\theta_{\max}^1 = 61^\circ$ and $\varphi_{\max}^1 = 90^\circ$. By applying a circular shift to the steering vector, one can obtain 12 different steering vectors, namely $\{V_{\max}^1, V_{\max}^2, \dots, V_{\max}^{12}\}$ and, consequently, also produce 12 different directions of the main beam shifted by the multiple of 30° (the explicit relation between V_{\max}^n and

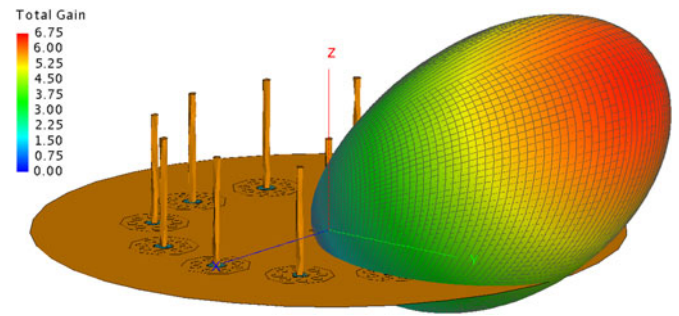


Fig. 2. ESPAR antenna's radiation pattern for one of its directional main beam configurations. The radiation pattern corresponds to the steering vector $V_{\max}^1 = [1, 1, 1, 1, 1, 0, 0, 0, 0, 0, 0, 0]$ and is provided by opening five neighboring passive elements, which are directors, while the others are reflectors shortened to the antenna ground (see text for explanations).

TABLE I
RADIATION PATTERNS DISCRETIZED IN THE HORIZONTAL PLANE ($\theta = 90^\circ$)
MEASURED FOR DIFFERENT STEERING VECTORS OF THE ESPAR ANTENNA

| n | V_{\max}^n | φ_{\max}^n | φ | | | | | | |
|-----|--------------|--------------------|-------------|-------------|------------|-----------|-----------|------------|------------|
| | | | -15° | -10° | -5° | 0° | 5° | 10° | 15° |
| 1 | 111110000000 | 90° | 0.13 | 0.15 | 0.18 | 0.22 | 0.26 | 0.33 | 0.41 |
| 2 | 011111000000 | 120° | 0.03 | 0.04 | 0.05 | 0.07 | 0.09 | 0.11 | 0.13 |
| 3 | 001111100000 | 150° | 0.02 | 0.02 | 0.02 | 0.02 | 0.02 | 0.02 | 0.03 |
| 4 | 000111110000 | 180° | 0.02 | 0.01 | 0.01 | 0.01 | 0.01 | 0.01 | 0.01 |
| 5 | 000011111000 | 210° | 0.03 | 0.03 | 0.02 | 0.02 | 0.02 | 0.02 | 0.01 |
| 6 | 000001111100 | 240° | 0.13 | 0.11 | 0.09 | 0.07 | 0.06 | 0.04 | 0.03 |
| 7 | 000000111110 | 270° | 0.41 | 0.33 | 0.27 | 0.22 | 0.18 | 0.15 | 0.13 |
| 8 | 000000011111 | 300° | 1.64 | 1.33 | 1.07 | 0.85 | 0.67 | 0.53 | 0.42 |
| 9 | 100000001111 | 330° | 3.81 | 3.49 | 3.13 | 2.74 | 2.35 | 1.98 | 1.64 |
| 10 | 110000000111 | 0° | 3.81 | 4.06 | 4.22 | 4.27 | 4.22 | 4.06 | 3.82 |
| 11 | 111000000011 | 30° | 1.64 | 1.98 | 2.35 | 2.74 | 3.13 | 3.49 | 3.80 |
| 12 | 111100000001 | 60° | 0.42 | 0.53 | 0.67 | 0.85 | 1.07 | 1.33 | 1.64 |

φ_{\max}^n can be found in Table I). It should be noted, however, that θ_{\max}^n will stay the same for all the considered steering vectors.

To analyze the proposed ESPAR antenna's radiation patterns in the horizontal plane, we will assume $\theta = 90^\circ$, which has been done by a majority of authors developing 1-D DoA estimation algorithms [1], [5], [6], [8]. Because, in the 12-element ESPAR antenna, the directional main beam can be switched by 30° , to analyze its radiation patterns, it is sufficient to focus on the directions falling within 30° wide angular span. This assumption allows one to present directional properties of the antenna in the horizontal plane in a convenient and legible way, which has been done in Table I for angles around $\varphi = 0^\circ$.

It can easily be seen that, in the results in Table I, there exists a strong diversity in radiation patterns' values in the horizontal plane for all the directions within the 30° span. In other words, assuming a signal impinging the antenna from an unknown horizontal angle, by switching the ESPAR antenna radiation patterns, for every direction, one will get a unique set of 12 RSS values recorded by the receiver. Thus, by a simple comparison of the obtained values with the previously recorded set, e.g., in a form similar to the one presented in Table I, one can perform 1-D DoA estimation in the horizontal plane.

To verify the possibility for simultaneous 1-D DoA estimation in the vertical plane using the proposed ESPAR antenna's

TABLE II
RADIATION PATTERNS DISCRETIZED IN THE VERTICAL PLANE ($\varphi = 0^\circ$)
MEASURED FOR DIFFERENT BEAM'S DIRECTIONS OF THE ESPAR ANTENNA

| n | φ_{\max}^n | θ | | | | | | | | |
|-----|--------------------|------------|------------|------------|------------|------------|------------|------------|------------|------------|
| | | 10° | 20° | 30° | 40° | 50° | 60° | 70° | 80° | 90° |
| 1 | 90° | 0.43 | 0.39 | 0.37 | 0.39 | 0.40 | 0.39 | 0.34 | 0.28 | 0.22 |
| 2 | 120° | 0.42 | 0.33 | 0.24 | 0.19 | 0.17 | 0.17 | 0.16 | 0.12 | 0.07 |
| 3 | 150° | 0.41 | 0.29 | 0.17 | 0.09 | 0.06 | 0.06 | 0.06 | 0.04 | 0.02 |
| 4 | 180° | 0.40 | 0.27 | 0.15 | 0.08 | 0.06 | 0.04 | 0.03 | 0.03 | 0.01 |
| 5 | 210° | 0.40 | 0.29 | 0.17 | 0.09 | 0.07 | 0.06 | 0.06 | 0.04 | 0.02 |
| 6 | 240° | 0.41 | 0.33 | 0.24 | 0.19 | 0.17 | 0.17 | 0.16 | 0.12 | 0.07 |
| 7 | 270° | 0.43 | 0.39 | 0.37 | 0.38 | 0.40 | 0.39 | 0.34 | 0.28 | 0.22 |
| 8 | 300° | 0.46 | 0.58 | 0.85 | 1.18 | 1.39 | 1.41 | 1.26 | 1.06 | 0.85 |
| 9 | 330° | 0.53 | 0.97 | 1.94 | 3.17 | 4.09 | 4.37 | 4.05 | 3.43 | 2.74 |
| 10 | 0° | 0.57 | 1.20 | 2.64 | 4.52 | 6.01 | 6.58 | 6.22 | 5.33 | 4.27 |
| 11 | 30° | 0.53 | 0.96 | 1.94 | 3.17 | 4.09 | 4.36 | 4.05 | 3.43 | 2.74 |
| 12 | 60° | 0.47 | 0.58 | 0.85 | 1.18 | 1.40 | 1.41 | 1.27 | 1.06 | 0.85 |

radiation patterns, one can perform an analogous reasoning as the one that has been done for the horizontal plane. To this end, discretized values of the designed ESPAR antenna radiation patterns for the plane $\varphi = 0^\circ$ were gathered in Table II. As it can easily be observed, the antenna exhibits diversity in radiation pattern's values also in the vertical plane. It means that by changing the main beam direction and recording RSS values of an unknown signal impinging the antenna, one not only can determine an unknown horizontal angle, but also a vertical one. Thus, this observation, not previously explored by others, may be used for RSS-based 2-D DoA estimation in both horizontal and vertical planes to naturally expand usefulness of the ESPAR antenna in practical DoA applications.

III. SIMPLE 2-D DOA ESTIMATION ALGORITHM

The results presented in Tables I and in II indicate that, assuming a signal impinging the proposed ESPAR antenna, by changing the antenna radiation patterns, one can determine not only DoA in the horizontal plane, but also its vertical plane counterpart. To implement the concept of 2-D DoA estimation, one may adapt the power pattern cross-correlation (PPCC) estimator introduced in [5] for 1-D DoA estimation in the horizontal plane. Exploiting the notation used herein, the 1-D DoA estimator is calculated using the following formula [8]:

$$\Gamma_{1D}(\varphi) = \frac{\sum_{n=1}^N (P(V_{\max}^n, \varphi) Y(V_{\max}^n))}{\sqrt{\sum_{n=1}^N P(V_{\max}^n, \varphi)^2} \sqrt{\sum_{n=1}^N Y(V_{\max}^n)^2}} \quad (1)$$

where N is the number of ESPAR antenna radiation patterns used, $\{Y(V_{\max}^1), Y(V_{\max}^2), \dots, Y(V_{\max}^N)\}$ are antenna output power values measured for the corresponding steering vectors $\{V_{\max}^1, V_{\max}^2, \dots, V_{\max}^N\}$, which set up the associated radiation patterns, and $\{P(V_{\max}^1, \varphi), P(V_{\max}^2, \varphi), \dots, P(V_{\max}^N, \varphi)\}$ are antenna power pattern values measured prior to the estimation for horizontal angle values φ varying from 0° to 360° with the angular step precision $\Delta\varphi$ and for all the corresponding steering vectors $\{V_{\max}^1, V_{\max}^2, \dots, V_{\max}^N\}$. The estimator $\Gamma_{1D}(\varphi)$ is, in fact, a correlation coefficient

between the power patterns $P(V_{\max}^n, \varphi)$ and an antenna output $\{Y(V_{\max}^1), Y(V_{\max}^2), \dots, Y(V_{\max}^N)\}$ measured for a signal impinging an ESPAR antenna. Because $\Gamma_{1D}(\varphi)$ values, obtained from (1), are calculated for all horizontal angle values φ , which were chosen prior to the actual estimation process during antenna power pattern $P(V_{\max}^n, \varphi)$ measurements for all considered steering vectors V_{\max}^n , the estimated 1-D horizontal DoA angle $\hat{\varphi}$ will correspond to the highest value of $\Gamma_{1D}(\varphi)$. The results reported in [5] indicate that, when $N = 6$ and power patterns $P(V_{\max}^n, \varphi)$ are measured with the angular step precision $\Delta\varphi = 1^\circ$, estimation of angle $\hat{\varphi}$ in the horizontal plane $\theta = 90^\circ$ can be performed with 0.67° estimation error mean.

To expand the above approach to include 2-D DoA estimation, we propose to introduce a new estimator $\Gamma_{2D}(\theta, \varphi)$ as a correlation coefficient between the power patterns and the recorded antenna output. Because the new estimator has to be calculated for horizontal angle values φ varying from 0° to 360° and vertical angle values θ varying from 0° to 90° , antenna power pattern values measured prior to the 2-D DoA estimation should be modified accordingly and take the form $P(V_{\max}^n, \theta, \varphi)$, where $\theta \in \langle 0^\circ, 90^\circ \rangle$ and $\varphi \in \langle 0^\circ, 360^\circ \rangle$. It means that for all steering vectors $\{V_{\max}^1, V_{\max}^2, \dots, V_{\max}^N\}$, one has to perform corresponding measurements of ESPAR antenna radiation patterns $\{P(V_{\max}^1, \theta, \varphi), \dots, P(V_{\max}^N, \theta, \varphi)\}$ with the angular step precisions $\Delta\theta$ and $\Delta\varphi$. In consequence, the proposed 2-D DoA estimator $\Gamma_{2D}(\theta, \varphi)$ can be written as

$$\Gamma_{2D}(\theta, \varphi) = \frac{\sum_{n=1}^N (P(V_{\max}^n, \theta, \varphi) Y(V_{\max}^n))}{\sqrt{\sum_{n=1}^N P(V_{\max}^n, \theta, \varphi)^2} \sqrt{\sum_{n=1}^N Y(V_{\max}^n)^2}} \quad (2)$$

Taking into account that $\Gamma_{2D}(\theta, \varphi)$ values in (2) are calculated for all directions $\theta \in \langle 0^\circ, 90^\circ \rangle$ and $\varphi \in \langle 0^\circ, 360^\circ \rangle$ with the angular step precisions $\Delta\theta$ and $\Delta\varphi$, respectively, the estimated vertical and horizontal DoA angles $\hat{\theta}$ and $\hat{\varphi}$ will now correspond to the highest value of the proposed 2-D DoA estimator $\Gamma_{2D}(\theta, \varphi)$.

IV. MEASUREMENTS

In order to verify the overall accuracy of the proposed 2-D DoA estimator $\Gamma_{2D}(\theta, \varphi)$, the fabricated ESPAR antenna has been measured in our $11.9 \times 5.6 \times 6.0$ -m³ anechoic chamber. In the initial step, all 12 ESPAR antenna radiation patterns $P(V_{\max}^n, \theta, \varphi)$ associated with 12 main beam directions have been measured at 2.484 GHz with angular step precisions $\Delta\theta = 5^\circ$ and $\Delta\varphi = 1^\circ$. Then, to examine DoA estimation accuracy, a signal generator within NI PXIe-5840 vector signal transceiver (VST) has been used to generate 10-dBm 2.484-GHz binary phase-shift keying (BPSK) test signal impinging the ESPAR antenna. The signal source has been placed in the same anechoic chamber 8.0 m from the ESPAR antenna with the same NI PXIe-5840 VST connected to ESPAR antenna's output to receive the BPSK test signal. To make the results easily comparable with those in [5] and [8], additive white Gaussian noise has been added to the received signal to generate a specific signal-to-noise ratio, and for every considered direction of an impinging signal, 10 ten snapshots were generated.

TABLE III
ESTIMATION ERRORS IN THE HORIZONTAL PLANE ($\hat{\varphi}_{\text{error}}$) AND IN THE
VERTICAL PLANE ($\hat{\theta}_{\text{error}}$) FOR THE PROPOSED 2-D DOA ESTIMATOR
 $\Gamma_{2D}(\theta, \varphi)$ AND THE DESIGNED 12-ELEMENT ESPAR ANTENNA

| θ_t | Horizontal plane error ($\hat{\varphi}_{\text{error}}$) | | | | Vertical plane error ($\hat{\theta}_{\text{error}}$) | | | |
|------------|---|--------------|--------------|-----------|--|--------|--------|-----------|
| | mean | rms | sth | precision | mean | rms | sth | precision |
| 90° | 1.86° | 2.23° | 1.25° | 4° | 4.31° | 6.51° | 4.95° | 15° |
| 80° | 1.19° | 1.48° | 0.89° | 3° | 2.22° | 3.73° | 3.03° | 10° |
| 70° | 1.28° | 1.73° | 1.19° | 5° | 3.19° | 6.29° | 5.50° | 25° |
| 60° | 1.56° | 2.05° | 1.36° | 5° | 1.53° | 3.00° | 2.62° | 10° |
| 50° | 1.25° | 1.72° | 1.20° | 5° | 3.19° | 4.93° | 3.81° | 10° |
| 40° | 1.89° | 2.39° | 1.49° | 6° | 3.19° | 5.20° | 4.17° | 15° |
| 30° | 2.81° | 3.59° | 2.28° | 8° | 13.06° | 21.70° | 17.58° | 50° |
| 20° | 2.61° | 3.51° | 2.38° | 8° | 2.78° | 6.01° | 5.40° | 25° |
| 10° | 7.33° | 8.73° | 4.81° | 22° | 1.94° | 3.12° | 2.47° | 5° |

The results in the bold text above (for $\theta_t = 90^\circ$ and horizontal plane error column) are equivalent to those presented in [5] (see text for explanations).

Signal's directions were chosen by rotating the receiving ESPAR antenna with a discreet angular step equal to 10° in both horizontal and vertical planes. Hence, the total number of 324 test pairs (θ_t, φ_t) has been considered with $\theta_t \in \{10^\circ, 20^\circ, \dots, 90^\circ\}$ for the elevation plane (nine values) and $\varphi_t \in \{0^\circ, 10^\circ, \dots, 350^\circ\}$ for the horizontal plane (36 values). For every impinging signal's direction (θ_t, φ_t), 12 RSS values have been recorded for all the main beam antenna configurations $\{Y(V_{\text{max}}^1), Y(V_{\text{max}}^2), \dots, Y(V_{\text{max}}^N)\}$, which are antenna output power values recorded for the corresponding steering vectors $\{V_{\text{max}}^1, V_{\text{max}}^2, \dots, V_{\text{max}}^N\}$.

Estimation errors for the proposed 2-D DoA estimator $\Gamma_{2D}(\theta, \varphi)$ are gathered in Table III. The results were produced in such a way that one can easily compare them with those available in [5] for the 1-D DoA horizontal plane ($\theta = 90^\circ$) PPCC estimator, where 0.67° estimation error mean and 2° precision have been measured for an ESPAR antenna having six parasitic elements. To this end, for $\text{SNR} = 20$ dB and at every considered vertical angle θ_t , absolute values of horizontal plane estimation errors were calculated for all tested horizontal directions $\varphi_t \in \{0^\circ, 10^\circ, \dots, 350^\circ\}$, and from these 36 values, estimation error mean, root-mean-square error, standard deviation, and precision, which after [5] and [8] is the biggest absolute error value obtained during DoA estimation, have been calculated. One should note, however, that by using 12 parasitic elements in the proposed design instead of six as in [5], computational complexity of such DoA estimation in the horizontal plane will be doubled. A similar procedure, in which absolute values of vertical plane estimation errors were calculated for all tested horizontal directions $\varphi_t \in \{0^\circ, 10^\circ, \dots, 350^\circ\}$, has been conducted to provide estimation errors in the vertical plane, which are available in the vertical plane error column of Table III.

The results indicate that by applying the 2-D DoA estimator $\Gamma_{2D}(\theta, \varphi)$, introduced in this letter, it is possible to estimate both elevation and horizontal angles by using the proposed ESPAR antenna and recorded RSS values only. Estimation errors in the horizontal plane for $\theta_t = 90^\circ$ are slightly bigger than those obtained in [5], which may be caused by using different an-

tenna radiation patterns in the horizontal plane due to different antenna designs. One should note, however, that the proposed approach uses simpler and more energy-efficient parasitic element switching method [8] than previously proposed in [5].

For lower θ_t values, one will obtain higher estimation errors in the horizontal plane due to changes that appear in the radiation patterns of the ESPAR antenna. In the vertical plane, the errors are higher than in the horizontal plane as the antenna radiation patterns were measured with different angular step precisions in both directions ($\Delta\theta = 5^\circ$ and $\Delta\varphi = 1^\circ$) and due to stronger diversity in the radiation patterns across the horizontal plane than along the vertical one, which can be observed in Tables I and II. Nevertheless, for vertical angles of impinging signals within the scope $\theta \in \langle 40^\circ, 90^\circ \rangle$, one may expect estimation error mean less than 1.89° in the horizontal plane and less than 4.31° in the vertical plane.

V. CONCLUSION

In the letter, a simple RSS-based 2-D DoA estimation algorithm has been proposed that can easily be applied to ESPAR antennas enhancing their DoA functionality. Exploiting the fact that by switching main beam ESPAR antenna radiation patterns, one obtains not only strong diversity in the horizontal direction but also a diversity in the vertical plane, it has been possible to perform 2-D DoA estimation for signals impinging an ESPAR antenna by relying solely on RSS values. In order to verify the overall accuracy of the proposed 2-D DoA estimator, $\Gamma_{2D}(\theta, \varphi)$, measurements have been performed. The results indicate that, for $\text{SNR} = 20$ dB, it is possible to estimate the direction of a signal impinging the antenna with 1.89° and 4.31° error mean in horizontal and vertical planes, respectively, for vertical angles of impinging signal falling in between 90° and 40° . Moreover, the new algorithm uses RSS-based values only; therefore, it can easily be applied in simple and inexpensive systems for 2-D DoA estimation, where the phase of impinging signals cannot easily be measured.

REFERENCES

- [1] S. Chandran, *Advances in Direction-of-Arrival Estimation*. London, U.K.: Artech House, 2005.
- [2] F. Viani, L. Lizzi, M. Donelli, D. Pregolato, G. Oliveri, and A. Massa, "Exploitation of parasitic smart antennas in wireless sensor networks," *J. Electromagn. Waves Appl.*, vol. 24, no. 7, pp. 993–1003, Jan. 2010.
- [3] R. Harrington, "Reactively controlled directive arrays," *IEEE Trans. Antennas Propag.*, vol. AP-26, no. 3, pp. 390–395, May 1978.
- [4] M. Rzymowski, P. Woznica, and L. Kulas, "Single-anchor indoor localization using ESPAR antenna," *IEEE Antennas Wireless Propag. Lett.*, vol. 15, pp. 1183–1186, 2016.
- [5] E. Taillefer, A. Hirata, and T. Ohira, "Direction-of-arrival estimation using radiation power pattern with an ESPAR antenna," *IEEE Trans. Antennas Propag.*, vol. 53, no. 2, pp. 678–684, Feb. 2005.
- [6] C. Plapous, J. Cheng, E. Taillefer, A. Hirata, and T. Ohira, "Reactance domain MUSIC algorithm for electronically steerable parasitic array radiator," *IEEE Trans. Antennas Propag.*, vol. 52, no. 12, pp. 3257–3264, Dec. 2004.
- [7] F. Roemer and M. Haardt, "Efficient 1-D and 2-D DOA estimation for non-circular sources with hexagonal shaped ESPAR arrays," in *Proc. IEEE Int. Conf. Acoust., Speech, Signal Process. Proc.*, Toulouse, France, 2006, pp. IV–IV.
- [8] L. Kulas, "Direction-of-arrival estimation using an ESPAR antenna with simplified beam steering," in *Proc. 47th Euro. Microw. Conf.*, Nuremberg, Germany, 2017, accepted for publication.